Therapeutic effect of pirfenidone in the sugen/hypoxia rat model of severe pulmonary hypertension

Paul-Benoit Poble, Carole Phan, Timothée Quatremare, Jennifer Bordenave, Raphaël Thuillet, Amélie Cumont, Alice Huertas, Ly Tu, Peter Dorfmüller, Marc Humbert, et al.

Therapeutic effect of pirfenidone in the Sugen/hypoxia rat model of severe pulmonary hypertension

[1,2,]Paul-Benoit Poble, [1,2]Carole Phan, [1,2]Timothée Quatremare, [1,2]Jennifer Bordenave, [1,2]Raphaël Thuillet, [1,2]Amélie Cumont, [1,2,3]Alice Huertas, [1, 2]Ly Tu, [1,2,4]Peter Dorfmüller, [1,2,3]Marc Humbert, [1,2,4]Maria-Rosa Ghigna, [1,2,3] Laurent Savale, [1,2#]Christophe Guignabert

[1]INSERM UMR_S 999, Le Plessis-Robinson, France; [2]Université Paris-Sud and Université Paris-Saclay, Kremlin-Bicêtre, France; [3]AP-HP, Service de Pneumologie, Centre de Référence de l'Hypertension Pulmonaire Sévère, DHU Thorax Innovation, Hôpital Bicêtre, France; [4]Pathology Department, Hôpital Marie Lannelongue, Le Plessis-Robinson, France.

[#]**Address correspondence to:** Christophe Guignabert, Ph.D; INSERM UMR_S 999; Hôpital Marie Lannelongue; 133, avenue de la Résistance; 92350 Le Plessis-Robinson, France. Tel: +33-1-40948833; Fax: +33-1-40942522; christophe.guignabert@inserm.fr

Running title: Pirfenidone attenuates severe PH in SuHx rats

Authors' contributions: Conception and design: PBP, LT, and CG; Analysis and interpretation: all; Drafting manuscript: PBP, CP, LT, MH, LS, and CG.

Funding footnote: This research was supported by grants from the French National Institute for Health and Medical Research (INSERM), the University of Paris-Sud and the University Paris-Saclay, the Marie Lannelongue Hospital, the French National Agency for Research (ANR) grant no. ANR-16-CE17-0014 (TAMIRAH), the Fondation de la Recherche Médicale (FRM) grant no. DEQ20150331712 (Equipe FRM 2015), and in part by the Département Hospitalo-Universitaire (DHU) Thorax Innovation (TORINO), the Assistance Publique-Hôpitaux de Paris (AP-HP), Service de Pneumologie, Centre de Référence de l'Hypertension Pulmonaire Sévère, the LabEx LERMIT (grant no ANR-10-LABX-0033), the French PAH patient association (HTAP France) and the french Fonds de Dotation "Recherche en Santé Respiratoire" - (FRSR) - Fondation du Souffle (FdS). PBP and CP are supported by the FRSR–FdS and JB is supported by the FRM.

Manuscript word count: 2834

"This article has an online data supplement, which is accessible from this issue's table of content online at www.atsjournals.org"

Scientific knowledge on the subject

- Progressive accumulation of extracellular matrix components and of vascular cells in the pulmonary arterial wall are hallmark pathogenic features of pulmonary arterial hypertension (PAH).
- Pirfenidone (5-methyl-1-phenyl-2-[1H]-pyridone or PFD) is an antifibrotic agent that has beneficial effects in patients with idiopathic pulmonary fibrosis (IPF), although its molecular target has not been elucidated.

What this study adds to the field

- Chronic treatment with PFD partially attenuates pulmonary artery smooth muscle cell (PA-SMC) proliferation and decreases matrix deposition, oxidative stress, and inflammatory cell infiltration in lungs of Sugen/Hypoxia (SuHx) rats with established PH.
- PFD dose-dependently decreases cell proliferation and migration in cultured human PA-SMCs derived from idiopathic PAH (iPAH) and attenuates their capacity to produce ECM components.
- PFD dose dependently enhanced FoxO1 protein levels in cultured human PA-SMCs and in SuHx-rats treated with PFD.

Non-standard Abbreviations:

8-oxo-dG = 8-oxo-deoxyguanosine
AT = acceleration time
AU = arbitrary unit
CO = cardiac output
Col = collagen
CTGF = connective tissue growth factor
DMSO = dimethyl sulfoxide
ECM = extracellular matrix
ET = ejection time
FCS = fetal calf serum
FoxO1 = forkhead box O1
iPAH = idiopathic pulmonary arterial hypertension
IPF = idiopathic pulmonary fibrosis
LV = left ventricle
mPAP = mean pulmonary arterial pressure
NS = not significant
PA-SMC = pulmonary artery smooth muscle cell
PAH = pulmonary arterial hypertension
PCNA = proliferating cell nuclear antigen
PDF = pirfenidone
PH = pulmonary hypertension
pSmad2/3 = phosphoSmad2/3
RV = right ventricle
S = septum
SOD2 = superoxide dismutase
SuHx = sugen/hypoxia
Tn-C = tenascin-C
TPVR = total pulmonary vascular resistance
TUNEL = deoxynucleotidyl transferase–mediated dUTP nick end-labeling
vWF = von Willebrand factor
α-SMA = alpha-smooth muscle actin
RHC = right heart catheterization.
TGF-β = transforming growth factor beta
DAPI = 4′,6-diamidino-2-phenylindole

Abstract

Rationale: Heightened pulmonary artery smooth muscle cell (PA-SMC) proliferation and migration and dynamic remodeling of the extracellular matrix (ECM) are hallmark pathogenic features of pulmonary arterial hypertension (PAH). Pirfenidone (PFD) is an orally bioavailable pyridone derivative with anti-fibrotic, anti-inflammatory and anti-oxidative properties currently used in the treatment of idiopathic pulmonary fibrosis (IPF).

Objectives: We therefore evaluate the efficacy of curative treatments with PFD in the Sugen/Hypoxia (SuHx) rat model of severe pulmonary hypertension (PH).

Measurements and Main Results: Treatment with PFD (30 mg/kg/day *per os* 3 times a day (t.i.d.) for 3 weeks) started 5 weeks after sugen injection partially reversed established PH, reducing total pulmonary vascular resistance, and structure. Consistent with these observations, we found that continued PFD treatment decreases PA-SMC proliferation and levels of extracellular matrix deposition in lungs and right ventricles in SuHx rats. Importantly, PFD attenuated the pro-proliferative and pro-migratory potentials of cultured PA-SMCs from patients with idiopathic PAH (iPAH) and their capacity to produce ECM components. Finally, we found that PFD dose dependently enhanced forkhead box (Fox)O1 protein levels and its nuclear translocation in cultured iPAH PA-SMCs and in PFD-treated SuHx rats.

Conclusions: PFD appears to be a potential therapy for PAH worthy of investigation and evaluation for clinical use in conjunction of current PAH treatments.

Word count: *211 words*

Keywords: *Pulmonary arterial hypertension • Pulmonary artery smooth muscle cell • Extracellular matrix • Pirfenidone • FoxO1*

Introduction

Pulmonary arterial hypertension (PAH) is characterized by a progressive pulmonary vascular remodeling of distal precapillary arteries that causes a significant increase of the right ventricle (RV) load, ultimately leading to right heart failure and premature death. Despite recent progresses, most patients still die from this pulmonary cardiovascular disorder or fail to respond adequately to medical therapy with a 5-years survival of 59% (1). Current treatments can relieve some PAH symptoms and slow the progress of PAH in some patients, but they have limited impact on the cellular and molecular mechanisms involved in the pathogenic pulmonary vascular remodeling. Among them, it is now well admitted that the dynamic and unadapted remodeling of the extracellular matrix remodeling (ECM) leads not only to qualitative and quantitative changes modulating vessel stiffness, but also forms a permissive milieu influencing cell motility, proliferation, apoptosis, and differentiation (2-5). Consistent with these notions, beneficial effects of different protease inhibitors have been reported in several animal models of pulmonary hypertension (6-10).

Pirfenidone (5-methyl-1-phenyl-2-[1H]-pyridone or PFD) is an orally available pyridone derivative with anti-fibrotic, anti-inflammatory and anti-oxidative properties currently used in the treatment of idiopathic pulmonary fibrosis (IPF) with a good safety and a proven efficacy on the decline of forced vital capacity in recent published multinational phase 3 trials (11-13). We therefore hypothesized that PFD could interfere with mechanism driving pulmonary vascular remodeling and thus contributing to slow down pulmonary hypertension (PH) in the Sugen/Hypoxia (SuHx) rat model. We investigated: **1)** the efficacy of PFD on pulmonary hemodynamics, pulmonary arteries thickness and right ventricular remodeling in the SuHx rat model of severe PH; **2)** whether or not chronic treatment with PFD affect the *in situ* ECM deposition as well as levels of oxidative stress, cell proliferation and of inflammatory cell infiltration in lungs of SuHx rats with established PH; **3)** whether or not PFD can be

considered as a potentially effective tool to handle the dysfunctional behavior of pulmonary artery smooth muscle cells (PA-SMCs) in PAH, particularly in the control of proliferation and/or migration of idiopathic PAH (iPAH) PA-SMCs as well as in their capacity to produce ECM components; **4)** the *in vitro* and *in vivo* effects of PFD on the expression patterns and activity levels of Smad2/3 and FoxO1, two nodes for signaling integration in PA-SMCs known to be involved in PH progression.

Methods

Animals and *in vivo* treatment

Young male Wistar rats (100 g, Janvier Labs, Saint Berthevin, France) received a single subcutaneous injection of SU5416 and were exposed to normobaric hypoxia for 3 weeks before to return to room air for 2 weeks. After PH establishment (5 weeks after injection of SU5416), pulsed-wave Doppler echocardiography was used to evaluate pulmonary artery acceleration time (AT) to ejection time (ET) ratio, using Vivid E9 (GE Healthcare, Velizy-Villacoublay, France). Then, the SuHx rats with established PH were randomly assigned to either: a vehicle control group (dimethyl sulfoxide (DMSO) diluted in water; 1:10) and a group that received PFD at a dose of 30 mg/kg/day *per os* 3 times a day (t.i.d.) for 3 weeks (**Figure 1A-B**) (14). At the end of these protocols, transthoracic echocardiography and right heart catheterisation were performed as previously described (15, 16). Briefly, animals were anesthetized with isoflurane. A polyvinyl catheter was introduced into the right jugular vein and pushed through the right ventricle into the pulmonary artery to measure the mean pulmonary arterial pressure (mPAP). Cardiac output (CO) in rats was measured using the thermodilution method. After measurement of hemodynamic parameters, the thorax was opened and the left lung immediately removed and frozen. The right lung was fixed in the

distended state by perfusion through the trachea with 4% formalin at a pressure of 20 cm H_20. The right ventricular hypertrophy was assessed by the Fulton Index and the percentage of wall thickness [(2 × medial wall thickness/ external diameter) × 100] and of muscularized vessels were performed.

Human PA-SMCs isolation, culture, and treatment

Primary human PA-SMCs were isolated from lung explants from iPAH patients or from lung specimens obtained during lobectomy or pneumonectomy at a distance from the tumor foci in control subjects. Preoperative echocardiography was performed in these control patients to rule out PH and the absence of tumoral infiltration was retrospectively established in all tissue sections by the histopathological analysis. Briefly, as previously described (16-18), small pieces of freshly isolated arteries were cultured in DMEM media supplemented with 15% of fetal calf serum (FCS), 2 mM L-glutamine and antibiotics. The isolated pulmonary PA-SMCs were strongly positive for alpha-smooth muscle actin (α-SMA), smooth muscle-specific SM22 protein and calponin and negative for von Willebrand factor and CD31. Cells were used at passage < 5. Cell proliferation was measured by 5-bromo-2-deoxyuridine (BrdU) incorporation using the DELFIA Cell proliferation kit (PerkinElmer, Courtaboeuf, France) and a time-resolved fluorometer EnVision™ Multilabel Reader (PerkinElmer). Cell migration was assessed using the *in vitro* wound-healing assay (Ibidi, Martinsried, Germany). Briefly, confluent monolayers of PASMCs were scratch wounded, and then incubated with complete media for 24h in presence or not of PFD at the indicated doses.

Western blot, and Immunostaining

Cells/tissues were homogenized and sonicated in RIPA buffer containing protease and phosphatase inhibitors and 30 µg of protein was used to detect tenascin (Tn)-C, collagen (col)1A, colV, fibronectin, phosphoSmad2/3 (pSmad2/3), FoxO1, nitrotyrosine, superoxide

dismutase (SOD)2, p21, catalase, connective tissue growth factor (CTGF) and β-actin (16-19). Immunohistochemistry and immunocytofluorescent staining for proliferating cell nuclear antigen (PCNA), CD45 (lymphocyte common antigen), CD68 (macrophage), 8-oxo-deoxyguanosine (8-oxo-dG), FoxO1, pSmad2/3, von Willebrand factor (vWF) and SM22 were performed in human and rat lung paraffin sections (16-19). Briefly, lung sections were deparaffined and stained with Hematoxylin and Eosin (Sigma-Aldrich, Saint-Quentin Fallavier, France), Picrosirius red, Masson's trichrome, or incubated with retrieval buffer. Then, sections were saturated with blocking buffer and incubated overnight with specific antibodies, followed by corresponding secondary fluorescent-labeled antibodies (Thermo Fisher Scientific, Saint-Aubin, France). Nuclei were labeled using DAPI (Thermo Fisher Scientific). Mounting was done using ProLong Gold antifade reagent (Thermo Fisher Scientific). Images were taken using LSM700 confocal microscope (Zeiss, Marly-le-Roi, France). Other lung sections were used for immunochemistry using vectastain ABC kit according to the manufacturer's instructions (Abcys, Courtaboeuf, France) and counterstained with Hematoxylin (Sigma-Aldrich). Images were taken using Eclipse 80i microscope (Nikon Instruments, Champigny-sur-Marne, France). We conducted terminal deoxynucleotidyl transferase–mediated dUTP nick end-labeling (TUNEL) using the ApopTag red in situ apoptosis detection kit (Chemicon, Molsheim, France).

Statistical analyses

Statistical significance was tested using the nonparametric Mann-Whitney U test, one- or two-way ANOVA with Bonferroni or Tukey post hoc tests, or Kruskal-Wallis test. Significant difference was assumed at a p value of < 0.05. Continuous data are expressed as mean ± SEM of at least three independent experiments or performed in triplicate or

quintuplicate for technical replicates. P value <0.05 was considered statistically significant. Analyses were performed using GraphPad Prism v5.0 (La Jolla, CA, USA).

Study approval

All animals were treated in accordance with the Guide for the Care and Use of Laboratory Animals as adopted by our National Institute of Health and Medical Research (INSERM) and approval was granted by the Ethics Committee of the University Paris-Sud, Le Plessis-Robinson, France. In addition, all the experiments with human specimens were approved by the local ethics committee (Comité de Protection des Personnes [CPP] Ile-de-France VII). All patients gave informed consent before the study.

Results

Efficacy of curative chronic treatment with PFD on the progression of PH in the Sugen/Hypoxia model in rats

First, we examined the effect of chronic PFD treatment against the progression of PH induced in rats by a single subcutaneous injection of sugen (SU5416; 20 mg/kg) followed by 3 weeks of hypoxia (10% FiO_2) and 2 weeks of normoxia. After PH establishment (five weeks after injection of sugen) rats were randomized and treated with PFD (30mg/kg t.i.d. by oral gavage (14)) or vehicle for 3 weeks (**Figure 1A-B**). On week-8, in SuHx rats treated with vehicle, a marked increase in mean pulmonary arterial pressure (mPAP), total pulmonary vascular resistance (TPVR), (**Figure 1C**), percentages of medial wall thickness and of muscularized distal pulmonary arteries (**Figure 2A**), and in RV/(LV+S) ratio (**Figure 2B**) were found compared with control rats. However, SuHx rats treated with PFD exhibited reduced TPVR with a less pronounced reduction in cardiac output (CO) when compared with vehicle-treated

SuHx rats (**Figure 1C**). Consistent with these results, the percentages of medial wall thickness and of muscularized distal pulmonary arteries were substantially decreased in SuHx rats treated with PFD when compared with vehicle-treated SuHx rats (**Figure 2A**). Interestingly, we also noted a reduced increase in cardiomyocyte cross-sectional area (CSA) and in collagen deposition in the right ventricle in SuHx rats treated with PFD when compared with vehicle-treated SuHx rats (**Figure 2B-C**). No significant differences were found in capillary density and small vessel density in the right ventricle between SuHx rats treated with PFD and vehicle-treated SuHx rats (**Figure 2D**). Of note, no differences were also found in values of heart rate (325 ± 22 *versus* 316 ± 18 bpm, respectively, NS) and systemic pressures (systemic blood pressure: 97 ± 7 *versus* 92 ± 8, respectively, NS) between SuHx rats treated with PFD and vehicle-treated SuHx rats.

Chronic treatment with PFD attenuates perivascular collagen deposition and reduces inflammation and oxidative stress in SuHx rat lungs

Since PFD has been shown to have anti-fibrotic, anti-inflammatory and anti-oxidant properties in several animal models of fibrosis in the lung, liver, kidney and heart (14), we next determined effects of PFD treatments on both the accumulation of ECM components, PA-SMCs and immune cells in lungs of SuHx rats treated or not with PFD (**Figure 3**). On week-8, a marked increased the percentage of perivascular collagen and of $PCNA^+$, $CD45^+$ and $CD68^+$ cells were found in lungs of in SuHx rats treated with vehicle when compared with controls (**Figure 3A-B, and 3D**). In contrast, both picrosirius red and Masson's trichrome staining indicate a substantial reduction in the percentage of perivascular collagen in lungs of PFD-treated SuHx rats when compared with vehicle-treated SuHx rats (**Figure 3A**). Consistent with our hemodynamic findings, numbers of $PCNA^+$ cells were decreased in pulmonary vessels of SuHx rats treated with PFD when compared with vehicle-treated SuHx rats, whereas numbers of $TUNEL^+$ cells were increased (**Figure 3B-C**), indicating a shift in

cell proliferation and apoptosis balance. In addition, we also found a reduction in the infiltration of $CD45^+$ and $CD68^+$ cells around vessels in lungs of SuHx rats treated with PFD (**Figure 3D**). Finally, we determined the effect of chronic PFD treatment on biomarkers of oxidative stress and found a substantial reduction in the level of oxidative DNA damage (8-oxo-dG) in lungs of PFD-treated SuHx rats when compared to vehicle-treated SuHx rats with and only a trend toward reduction of oxidative protein damage (nitrotyrosine) (**Figure 3E-F**).

Pirfenidone attenuates the pro-proliferative and pro-migratory phenotypes of cultured PA-SMCs derived from idiopathic PAH (iPAH) patients in a dose dependent manner

Both PA-SMC proliferation and migration played major contribution to the progression of pulmonary vascular remodeling in PAH (neo-intima formation and media hypertrophy) (16, 17), we next examined the effect of PFD treatment on the proliferative and migratory potentials of cultured PA-SMCs derived from iPAH patients. PFD, at either low or high dose, had no obvious effect on cell morphology or viability (**Supplemental Fig. 1A**). However, we found that high doses of PFD reduced iPAH PA-SMC proliferation (**Figure 4A**) and migration in the well-established 2D scratch assay (**Figure 4B**). We also found that even if high doses of PFD is associated with qualitative and quantitative changes in ECM components, characterized by an increase in Tn-C and substantial reductions in the production of col1A, colV and fibronectin (**Figure 4C**).

Pirfenidone increases FoxO1 expression and nuclear localization in iPAH PA-SMCs

Since FoxO1 isoform inactivation is known to be central for the pro-proliferative and apoptosis-resistant phenotype in iPAH PA-SMCs and a major downstream mediator of growth factors and inflammatory cytokines (20), we studied whether PFD regulates FoxO1 expression and/or activity. Interestingly, a dose-dependent increase in FoxO1 protein levels was found in iPAH PA-SMCs exposed to PFD (**Figure 5A**). Consistent with this observation,

immunofluorescence and confocal analysis validates that PFD increases FoxO1 nuclear localization in iPAH PA-SMCs (**Figure 5B**). In addition, we found that exposure of iPAH PA-SMCs to PFD increases protein expression levels of three FoxO1 targets, namely p21, SOD2, and catalase (**Figure 5C**).

We next conducted parallel evaluations to determine whether PFD-induced upregulation of nuclear FoxO1 is involved in the attenuation of the pro-proliferative phenotype in iPAH PA-SMCs. To this aim, iPAH PA-SMCs were exposed to PFD in presence or not of AS1842856, a cell-permeable FoxO1 inhibitor that blocks the transcription activity of FoxO1. The results of our bromodeoxyuridine (BrdU) incorporation studies indicate that treatment with AS1842856 attenuates the inhibitory effect of PFD on iPAH PA-SMCs (**Figure 5D**).

These *in vitro* observations were replicated *in vivo*, with a stronger immunoreactivity of FoxO1 in the smooth muscle of pulmonary vessels of PFD-treated SuHx rats when compared to vehicle-treated SuHx rats (**Figure 6A**). Western blot analyses confirmed upregulation of FoxO1 protein in lung homogenates of PFD-treated SuHx rats (**Figure 6B**).

Recent studies support the notion that FoxO family members act synergistically with the TGF-β1 signaling pathway to promote gene expression of many targets in fibroblasts (21-23). Subsequent *in vitro* studies were therefore performed to study the effects of PFD treatment on the TGF-β1 signaling pathway in iPAH PA-SMCs. Consistent with this notion, we found that high doses of PFD decreases levels of pSmad2/3 and CTGF a downstream target of the TGF-β1 in iPAH PA-SMCs (**Supplemental Fig. 1B**). Although TGF-β1 increases pSmad2/3 nuclear localization, TGF-β1 has no effect on FoxO1 nuclear localization in iPAH PA-SMCs and do not interfere with the PFD-induced upregulation of nuclear FoxO1 (**Supplemental Figure 1C**).

Discussion

Although PFD displays anti-inflammatory, anti-fibrotic, and anti-oxidant properties both *in vitro* and in animal models of pulmonary fibrosis, its efficacy against the progression of the pulmonary vascular remodeling in SuHx rats has never been tested. Herein, we demonstrate that chronic treatment with PFD partially attenuates PA-SMC proliferation and decreases ECM deposition, oxidative stress, and inflammatory cell infiltration in lungs of Sugen/Hypoxia (SuHx) rats with established PH. In addition, we found that PFD dose-dependently attenuates cell proliferation and migration in cultured human PA-SMCs derived from iPAH patients and their capacity to produce ECM components. Finally, we reported that PFD dose dependently enhanced FoxO1 protein levels in cultured human PA-SMCs and in SuHx rats treated with PFD.

Several preclinical studies have demonstrated that chronic treatment with PFD has beneficial effects of in the bleomycin model of pulmonary fibrosis and that a dose of 30 mg/kg/day t.i.d. *per os* can be considered as an intermediate dose that is clinically relevant (14). Although there were no significant decreased in the values of mPAP and Fulton index in this animal model of severe PH, we interestingly found that chronic PFD administration in SuHx rats with established PH significantly decrease TPVR values and reduce the progression of pulmonary vascular remodeling. Consistent with these beneficial effects of chronic PFD treatment on cardiac functions in our SuHx rats, we found a marked attenuation of the collagen deposition in the right ventricle in these animals when compared with vehicle-treated SuHx rats. Although extracellular matrix deposition in the RV is well known to lead to elevated ventricular stiffness and the development of heart failure (24, 25), it is less known to which extent it could affects RV mass in rats with severe PH. Since we cannot exclude that this beneficial effect of PFD treatments on the right ventricle is an indirect action, additional work is needed to study the potential effect of chronic treatment with PFD in a rat model of

increased right ventricular afterload induced by pulmonary artery banding. Indeed, several accumulating evidences are supporting that PFD has direct beneficial actions on left ventricular remodeling and functions in several animal models (26-29).

The molecular mechanism underlying the protective effects of PFD in pulmonary fibrosis remains unknown, however our findings indicate that PFD treatment increases FoxO1 expression and nuclear localization *in vivo* and *in vitro* in cultured PA-SMCs derived from iPAH patients. Interestingly, the effect of PFD on the nuclear translocation of FoxO1 in iPAH PA-SMCs is more pronounced that those observed on the nuclear translocation of pSmad2/3. Since recent studies support the notion that FoxO family members act synergistically with the TGF-β1 signaling pathway to promote gene expression of many targets in fibroblasts (21-23), it would be interesting to follow the impact of PFD on the induced fibroblast- to-myofibroblast transition in human lung fibroblast populations. Interestingly, we found that high doses of PFD decreases pSmad2/3 levels in iPAH PA-SMCs and CTGF protein expression. A recent study has also suggest that PFD exerts its clinically beneficial effects through dual hedgehog (hh)/TGF-β inhibition by targeting the GLI2 protein. Interestingly, Foxc1 is an important transcriptional partner of indian hedgehog (Ihh)/Gli2 signaling during endochondral ossification (30), however whether FoxO1 is necessary for the Ihh-Gli2 signaling is still unknown. Importantly, we found that PFD has the ability of attenuating the pro-proliferative and pro-migratory phenotype of iPAH PA-SMCs. Furthermore, high doses of PFD reduces the production of several ECM components in iPAH PA-SMCs *in vitro* and in lungs and the right ventricle of SuHx rats. Since each animal models is different and mimics only some parts of the human condition (31), substantial work remains to be done to validate the role of this reactivation of endogenous FoxO1 in PH using different doses of PFD in other animal models. However, because PH is a common complication of IPF that significantly contributes to morbidity and mortality (32), our present findings encourage the

evaluation of PFD on pulmonary hemodynamics in patients with this IPF-PH. This notion is particularly relevant in the light of the fact that nintedanib has been recently reported to have disadvantageous effects in experimental and human PAH (33).

In summary, these findings underline that chronic treatments with PFD at clinical relevant doses can partially reverse severe PH in SuHx rats. Our data indicate that this beneficial effect is mediated not only by a decrease in PA-SMC proliferation and migration, but also by reduction of oxidative stress levels and inflammatory cell infiltration in lungs of PFD-treated SuHx rats. Our data also indicate that PFD can positively affect FoxO1 a master signaling integrator that is known to be central for the PA-SMC accumulation during the progression of PAH. Our findings should encourage clinical investigations and especially the evaluation of the use of PFD in conjunction with current PAH therapies.

Conflict of interest

None.

Disclosures

PBP, CP, TQ, JB, RT, AC, AH, LT, PD, MRG, and CG have no conflicts of interest to disclose. In the past 3 years, MH and LS report grants, personal fees, and nonfinancial support from Actelion, Pfizer, Bayer, and GlaxoSmithKline, MSD, outside of the submitted work.

References:

1. Boucly, A., Weatherald, J., Savale, L., Jais, X., Cottin, V., Prevot, G., Picard, F., de Groote, P., Jevnikar, M., Bergot, E., Chaouat, A., Chabanne, C., Bourdin, A., Parent, F., Montani, D., Simonneau, G., Humbert, M., and Sitbon, O. (2017) Risk assessment, prognosis and guideline implementation in pulmonary arterial hypertension. *Eur Respir J* **50**
2. Bertero, T., Oldham, W. M., Cottrill, K. A., Pisano, S., Vanderpool, R. R., Yu, Q., Zhao, J., Tai, Y., Tang, Y., Zhang, Y. Y., Rehman, S., Sugahara, M., Qi, Z., Gorcsan, J., 3rd, Vargas, S. O., Saggar, R., Saggar, R., Wallace, W. D., Ross, D. J., Haley, K. J., Waxman, A. B., Parikh, V. N., De Marco, T., Hsue, P. Y., Morris, A., Simon, M. A., Norris, K. A., Gaggioli, C., Loscalzo, J., Fessel, J., and Chan, S. Y. (2016) Vascular stiffness mechanoactivates YAP/TAZ-dependent glutaminolysis to drive pulmonary hypertension. *J Clin Invest* **126**, 3313-3335
3. Huertas, A., Tu, L., and Guignabert, C. (2017) New targets for pulmonary arterial hypertension: going beyond the currently targeted three pathways. *Curr Opin Pulm Med* **23**, 377-385
4. Avouac, J., Guignabert, C., Hoffmann-Vold, A. M., Ruiz, B., Dorfmuller, P., Pezet, S., Amar, O., Tu, L., Van Wassenhove, J., Sadoine, J., Launay, D., Elhai, M., Cauvet, A., Subramaniam, A., Resnick, R., Hachulla, E., Molberg, O., Kahan, A., Humbert, M., and Allanore, Y. (2017) Role of Stromelysin 2 (Matrix Metalloproteinase 10) as a Novel Mediator of Vascular Remodeling Underlying Pulmonary Hypertension Associated With Systemic Sclerosis. *Arthritis Rheumatol* **69**, 2209-2221
5. Guignabert, C., Tu, L., Girerd, B., Ricard, N., Huertas, A., Montani, D., and Humbert, M. (2015) New molecular targets of pulmonary vascular remodeling in pulmonary arterial hypertension: importance of endothelial communication. *Chest* **147**, 529-537
6. Maruyama, K., Ye, C. L., Woo, M., Venkatacharya, H., Lines, L. D., Silver, M. M., and Rabinovitch, M. (1991) Chronic hypoxic pulmonary hypertension in rats and increased elastolytic activity. *Am J Physiol* **261**, H1716-1726
7. Cowan, K. N., Heilbut, A., Humpl, T., Lam, C., Ito, S., and Rabinovitch, M. (2000) Complete reversal of fatal pulmonary hypertension in rats by a serine elastase inhibitor. *Nature medicine* **6**, 698-702

8. Zaidi, S. H., You, X. M., Ciura, S., Husain, M., and Rabinovitch, M. (2002) Overexpression of the serine elastase inhibitor elafin protects transgenic mice from hypoxic pulmonary hypertension. *Circulation* **105**, 516-521
9. Ilkiw, R., Todorovich-Hunter, L., Maruyama, K., Shin, J., and Rabinovitch, M. (1989) SC-39026, a serine elastase inhibitor, prevents muscularization of peripheral arteries, suggesting a mechanism of monocrotaline-induced pulmonary hypertension in rats. *Circulation research* **64**, 814-825
10. Vieillard-Baron, A., Frisdal, E., Raffestin, B., Baker, A. H., Eddahibi, S., Adnot, S., and D'Ortho, M. P. (2003) Inhibition of matrix metalloproteinases by lung TIMP-1 gene transfer limits monocrotaline-induced pulmonary vascular remodeling in rats. *Human gene therapy* **14**, 861-869
11. Noble, P. W., Albera, C., Bradford, W. Z., Costabel, U., du Bois, R. M., Fagan, E. A., Fishman, R. S., Glaspole, I., Glassberg, M. K., Lancaster, L., Lederer, D. J., Leff, J. A., Nathan, S. D., Pereira, C. A., Swigris, J. J., Valeyre, D., and King, T. E., Jr. (2016) Pirfenidone for idiopathic pulmonary fibrosis: analysis of pooled data from three multinational phase 3 trials. *Eur Respir J* **47**, 243-253
12. Noble, P. W., Albera, C., Bradford, W. Z., Costabel, U., Glassberg, M. K., Kardatzke, D., King, T. E., Jr., Lancaster, L., Sahn, S. A., Szwarcberg, J., Valeyre, D., du Bois, R. M., and Group, C. S. (2011) Pirfenidone in patients with idiopathic pulmonary fibrosis (CAPACITY): two randomised trials. *Lancet* **377**, 1760-1769
13. King, T. E., Jr., Bradford, W. Z., Castro-Bernardini, S., Fagan, E. A., Glaspole, I., Glassberg, M. K., Gorina, E., Hopkins, P. M., Kardatzke, D., Lancaster, L., Lederer, D. J., Nathan, S. D., Pereira, C. A., Sahn, S. A., Sussman, R., Swigris, J. J., Noble, P. W., and Group, A. S. (2014) A phase 3 trial of pirfenidone in patients with idiopathic pulmonary fibrosis. *N Engl J Med* **370**, 2083-2092
14. Schaefer, C. J., Ruhrmund, D. W., Pan, L., Seiwert, S. D., and Kossen, K. (2011) Antifibrotic activities of pirfenidone in animal models. *Eur Respir Rev* **20**, 85-97
15. Guignabert, C., Phan, C., Seferian, A., Huertas, A., Tu, L., Thuillet, R., Sattler, C., Le Hiress, M., Tamura, Y., Jutant, E. M., Chaumais, M. C., Bouchet, S., Maneglier, B., Molimard, M., Rousselot, P., Sitbon, O., Simonneau, G., Montani, D., and Humbert, M. (2016) Dasatinib induces lung vascular toxicity and predisposes to pulmonary hypertension. *J Clin Invest* **126**, 3207-3218
16. Tamura, Y., Phan, C., Tu, L., Le Hiress, M., Thuillet, R., Jutant, E. M., Fadel, E., Savale, L., Huertas, A., Humbert, M., and Guignabert, C. (2018) Ectopic upregulation

of membrane-bound IL6R drives vascular remodeling in pulmonary arterial hypertension. *J Clin Invest* **128**, 1956-1970

17. Tu, L., De Man, F. S., Girerd, B., Huertas, A., Chaumais, M. C., Lecerf, F., Francois, C., Perros, F., Dorfmuller, P., Fadel, E., Montani, D., Eddahibi, S., Humbert, M., and Guignabert, C. (2012) A critical role for p130Cas in the progression of pulmonary hypertension in humans and rodents. *Am J Respir Crit Care Med* **186**, 666-676
18. Huertas, A., Tu, L., Thuillet, R., Le Hiress, M., Phan, C., Ricard, N., Nadaud, S., Fadel, E., Humbert, M., and Guignabert, C. (2015) Leptin signalling system as a target for pulmonary arterial hypertension therapy. *Eur Respir J* **45**, 1066-1080
19. Tu, L., Dewachter, L., Gore, B., Fadel, E., Dartevelle, P., Simonneau, G., Humbert, M., Eddahibi, S., and Guignabert, C. (2011) Autocrine fibroblast growth factor-2 signaling contributes to altered endothelial phenotype in pulmonary hypertension. *Am J Respir Cell Mol Biol* **45**, 311-322
20. Savai, R., Al-Tamari, H. M., Sedding, D., Kojonazarov, B., Muecke, C., Teske, R., Capecchi, M. R., Weissmann, N., Grimminger, F., Seeger, W., Schermuly, R. T., and Pullamsetti, S. S. (2014) Pro-proliferative and inflammatory signaling converge on FoxO1 transcription factor in pulmonary hypertension. *Nat Med* **20**, 1289-1300
21. Vivar, R., Humeres, C., Munoz, C., Boza, P., Bolivar, S., Tapia, F., Lavandero, S., Chiong, M., and Diaz-Araya, G. (2016) FoxO1 mediates TGF-beta1-dependent cardiac myofibroblast differentiation. *Biochim Biophys Acta* **1863**, 128-138
22. Yadav, H., Devalaraja, S., Chung, S. T., and Rane, S. G. (2017) TGF-beta1/Smad3 Pathway Targets PP2A-AMPK-FoxO1 Signaling to Regulate Hepatic Gluconeogenesis. *J Biol Chem* **292**, 3420-3432
23. Al-Tamari, H. M., Dabral, S., Schmall, A., Sarvari, P., Ruppert, C., Paik, J., DePinho, R. A., Grimminger, F., Eickelberg, O., Guenther, A., Seeger, W., Savai, R., and Pullamsetti, S. S. (2018) FoxO3 an important player in fibrogenesis and therapeutic target for idiopathic pulmonary fibrosis. *EMBO Mol Med* **10**, 276-293
24. Egemnazarov, B., Crnkovic, S., Nagy, B. M., Olschewski, H., and Kwapiszewska, G. (2018) Right ventricular fibrosis and dysfunction: Actual concepts and common misconceptions. *Matrix Biol* **68-69**, 507-521
25. Golob, M. J., Wang, Z., Prostrollo, A. J., Hacker, T. A., and Chesler, N. C. (2016) Limiting collagen turnover via collagenase-resistance attenuates right ventricular dysfunction and fibrosis in pulmonary arterial hypertension. *Physiol Rep* **4**

26. Wang, Y., Wu, Y., Chen, J., Zhao, S., and Li, H. (2013) Pirfenidone attenuates cardiac fibrosis in a mouse model of TAC-induced left ventricular remodeling by suppressing NLRP3 inflammasome formation. *Cardiology* **126**, 1-11
27. Lee, K. W., Everett, T. H. t., Rahmutula, D., Guerra, J. M., Wilson, E., Ding, C., and Olgin, J. E. (2006) Pirfenidone prevents the development of a vulnerable substrate for atrial fibrillation in a canine model of heart failure. *Circulation* **114**, 1703-1712
28. Nguyen, D. T., Ding, C., Wilson, E., Marcus, G. M., and Olgin, J. E. (2010) Pirfenidone mitigates left ventricular fibrosis and dysfunction after myocardial infarction and reduces arrhythmias. *Heart Rhythm* **7**, 1438-1445
29. Mirkovic, S., Seymour, A. M., Fenning, A., Strachan, A., Margolin, S. B., Taylor, S. M., and Brown, L. (2002) Attenuation of cardiac fibrosis by pirfenidone and amiloride in DOCA-salt hypertensive rats. *Br J Pharmacol* **135**, 961-968
30. Yoshida, M., Hata, K., Takashima, R., Ono, K., Nakamura, E., Takahata, Y., Murakami, T., Iseki, S., Takano-Yamamoto, T., Nishimura, R., and Yoneda, T. (2015) The transcription factor Foxc1 is necessary for Ihh-Gli2-regulated endochondral ossification. *Nat Commun* **6**, 6653
31. Bonniaud, P., Fabre, A., Frossard, N., Guignabert, C., Inman, M., Kuebler, W. M., Maes, T., Shi, W., Stampfli, M., Uhlig, S., White, E., Witzenrath, M., Bellaye, P. S., Crestani, B., Eickelberg, O., Fehrenbach, H., Guenther, A., Jenkins, G., Joos, G., Magnan, A., Maitre, B., Maus, U. A., Reinhold, P., Vernooy, J. H. J., Richeldi, L., and Kolb, M. (2018) Optimising experimental research in respiratory diseases: an ERS statement. *Eur Respir J* **51**
32. Simonneau, G., Gatzoulis, M. A., Adatia, I., Celermajer, D., Denton, C., Ghofrani, A., Gomez Sanchez, M. A., Krishna Kumar, R., Landzberg, M., Machado, R. F., Olschewski, H., Robbins, I. M., and Souza, R. (2013) Updated clinical classification of pulmonary hypertension. *J Am Coll Cardiol* **62**, D34-41
33. Richter, M. J., Ewert, J., Grimminger, F., Ghofrani, H. A., Kojonazarov, B., Petrovic, A., Seeger, W., Schermuly, R. T., Tello, K., and Gall, H. (2018) Nintedanib in Severe Pulmonary Arterial Hypertension. *Am J Respir Crit Care Med*

Figure Legend:

***Figure 1*: Chronic curative treatments with pirfenidone (PFD) partially reverse pulmonary hypertension (PH) in Sugen Hypoxia (SuHx) rats.** **(A)** Experimental strategy used to test the efficacy of PFD in the SuHx rat model of severe PH. **(B)** Acceleration time (AT)/ejection time (ET) ratio obtained by transthoracic echocardiography (n=5-6). **(C)** Pulmonary hemodynamic parameters: mean pulmonary arterial pressure (mPAP), cardiac output (CO), and total pulmonary vascular resistance (TPVR) in control and SuHx rats treated with vehicle or PFD (30 mg/kg t.i.d. by oral gavage). Values are means±SEM (n=4-6). Comparisons were made using the one- or two-way ANOVA with Bonferroni's post hoc tests. **p<0.01, ***p<0.001, ****p<0.0001 *versus* controls rats; #p<0.05, ##p<0.01 *versus* SuHx rats. AU = arbitrary unit; ns = not significant; RHC = right heart catheterization.

***Figure 2*: Chronic curative treatments with pirfenidone (PFD) attenuate pulmonary vascular and right ventricular (RV) remodeling in Sugen Hypoxia (SuHx) rats.** **(A)** Representative images of H&E and α-smooth muscle actin (α-SMA) immunostaining, and quantification of the percentage of wall thickness and of muscularized distal pulmonary arteries in lungs of control and SuHx rats treated with vehicle or PFD. **(B)** Representative images of H&E staining of tissue section of right ventricle myocardium of control and SuHx rats treated with vehicle or PFD, Fulton index, and quantification of cardiomyocyte cross-sectional area. Representative images and quantifications of picrosirius and Masson's trichrome **(C)**, and of CD31 staining **(D)** in tissue section of right ventricle myocardium of control and SuHx rats treated with vehicle or PFD. Scale bar = 50 µm in all sections. Values are means±SEM (n=3-6). Comparisons were made using the one-way ANOVA with Bonferroni's post hoc tests. *p<0.05, **p<0.01, ***p<0.001, ****p<0.0001 *versus* controls rats; #p<0.05, ###p<0.001, ####p<0.0001 *versus* SuHx rats. AU = arbitrary unit; ns = not significant.

***Figure 3*: Chronic treatments with pirfenidone (PFD) exhibit anti-fibrotic, anti-inflammatory and anti-oxidative properties in lungs of Sugen Hypoxia (SuHx) rats.** Representative images and quantifications of picrosirius red and Masson's trichrome **(A)**, PCNA **(B)**, and TUNEL **(C)**, CD45 and CD68 staining **(D)**, and of 8-oxo-deoxyguanosine (8-oxo-dG) **(E)** in lungs of control and SuHx rats treated with vehicle or PFD (n=3-6). **(F)** Representative Western blots and quantification of the nitrotyrosine:β-actin ratio in lungs of control, vehicle- and PFD-treated rats. Values are means±SEM (n=3-9). Scale bar = 50 µm in all sections. Comparisons were made using the one-way ANOVA with Bonferroni's post hoc tests. *p<0.05, **p<0.01, ***p<0.001, ****p<0.0001 *versus* controls rats; #p<0.05, ##p<0.01 *versus* SuHx rats. AU = arbitrary unit; ns = not significant, TUNEL = terminal deoxynucleotidyl transferase dUTP nick end labeling.

***Figure 4*: Pirfenidone (PFD) attenuates the pro-proliferative and pro-migratory phenotypes of cultured PA-SMCs derived from idiopathic PAH (iPAH) patients in a dose dependent manner.** **(A)** 5-bromo-2-deoxyuridine (BrdU) incorporation in iPAH PA-SMCs under basal condition (0% fetal calf serum or FCS) or in response to increasing doses of PFD in presence of 10% FCS. **(B)** PA-SMC migration in response to increasing doses of PFD in presence of 10% FCS assessed with the *in vitro* wound-healing assay. Images of wounded monolayer of PA-SMCs were taken at times 0, 8, 12, and 24 h after treatment with PFD. The horizontal lines indicate the wound edge. **(C)** Representative Western blots and quantification of the collagen (Col)1A:β-actin, the colV:β-actin, the fibronectin (Fn):β-actin, and the tenascin (Tn)-C:β-actin ratios in iPAH PA-SMCs exposed to increased doses of PFD for 48 hours. Values are means±SEM (n=4-7). Comparisons were made using the one-way ANOVA

with Tukey's post hoc tests. *p<0.05, **p<0.01, ***p<0.001 *versus* cells without PFD in presence of 10% FCS. #p<0.05 *versus* other conditions.

***Figure 5*: Pirfenidone (PFD) increases forkhead box protein (Fox)O1 expression and nuclear localization in iPAH PA-SMCs.** **(A)** Representative Western blots and quantification of the FoxO1:GAPDH ratio in PA-SMCs from idiopathic PAH (iPAH) patients treated with increasing doses of PFD during 48h. Comparisons were made using the nonparametric one-way ANOVA with Kruskal-Wallis tests. **(B)** Double staining for FoxO1 and DAPI in iPAH PA-SMCs treated or not with PFD (1mg/mL) during 48h and percentages of FoxO1colocalization with DAPI. Comparisons were made using the nonparametric Mann-Whitney U test. **(C)** Representative Western blots and quantification of the FoxO1:GAPDH, p21:GAPDH, catalase:GAPDH, and superoxide dismutase (SOD)2:GAPDH ratios in iPAH PA-SMCs treated or not with the high dose of PFD during 24h. **(D)** 5-bromo-2-deoxyuridine (BrdU) incorporation in iPAH PA-SMCs under basal condition (0% fetal calf serum or FCS) or in response to increasing to PFD (1mg/mL) with or without the FoxO1 inhibitor AS1842856 (0.3µM). Comparisons were made using the nonparametric Mann-Whitney U test or using the one-way Repeated Measures ANOVA with Bonferroni's post hoc tests. Values are means±SEM (n=5-9). *p<0.05, **p<0.01, ****p<0.0001 *versus* control without PFD or basal condition. #p<0.05, ##p<0.01 *versus* other conditions.

***Figure 6*: Pirfenidone (PFD) increases forkhead box protein (Fox)O1 expression and nuclear localization in lungs of Sugen Hypoxia (SuHx) rats.** **(A)** Double staining for FoxO1 with SM22 and DAPI in lungs of control and SuHx rats treated with vehicle or PFD. **(B)** Representative Western blots and quantification of the FoxO1:GAPDH, ratio in lungs of control and SuHx rats treated with vehicle or PFD. Comparisons were made using the one-way Repeated Measures ANOVA with Bonferroni's post hoc tests. Values are means±SEM (n=4-7). ****p<0.0001 *versus* control without PFD or basal condition. ##p<0.01 *versus* other conditions.

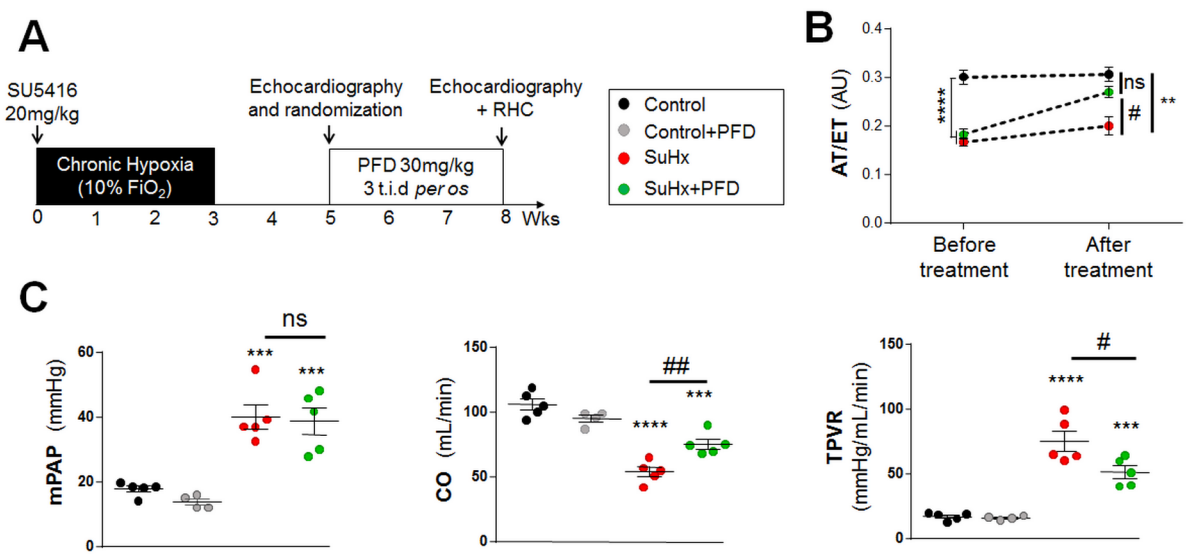
A
SU5416
20mg/kg
Chronic Hypoxia
(10% FiO2)
Echocardiography
and randomization
Echocardiography
+ RHC
PFD 30mg/kg
3 t.i.d per os
0 1 2 3 4 5 6 7 8 Wks
Control
Control+PFD
SuHx
SuHx+PFD
B
AT/ET (AU)
0.4
0.3
0.2
0.1
0.0
****
ns
#
**
Before
treatment
After
treatment
C
mPAP (mmHg)
60
40
20
0
ns
***
***
CO (mL/min)
150
100
50
0
##
****
***
TPVR
(mmHg/mL/min)
150
100
50
0
#
****
***

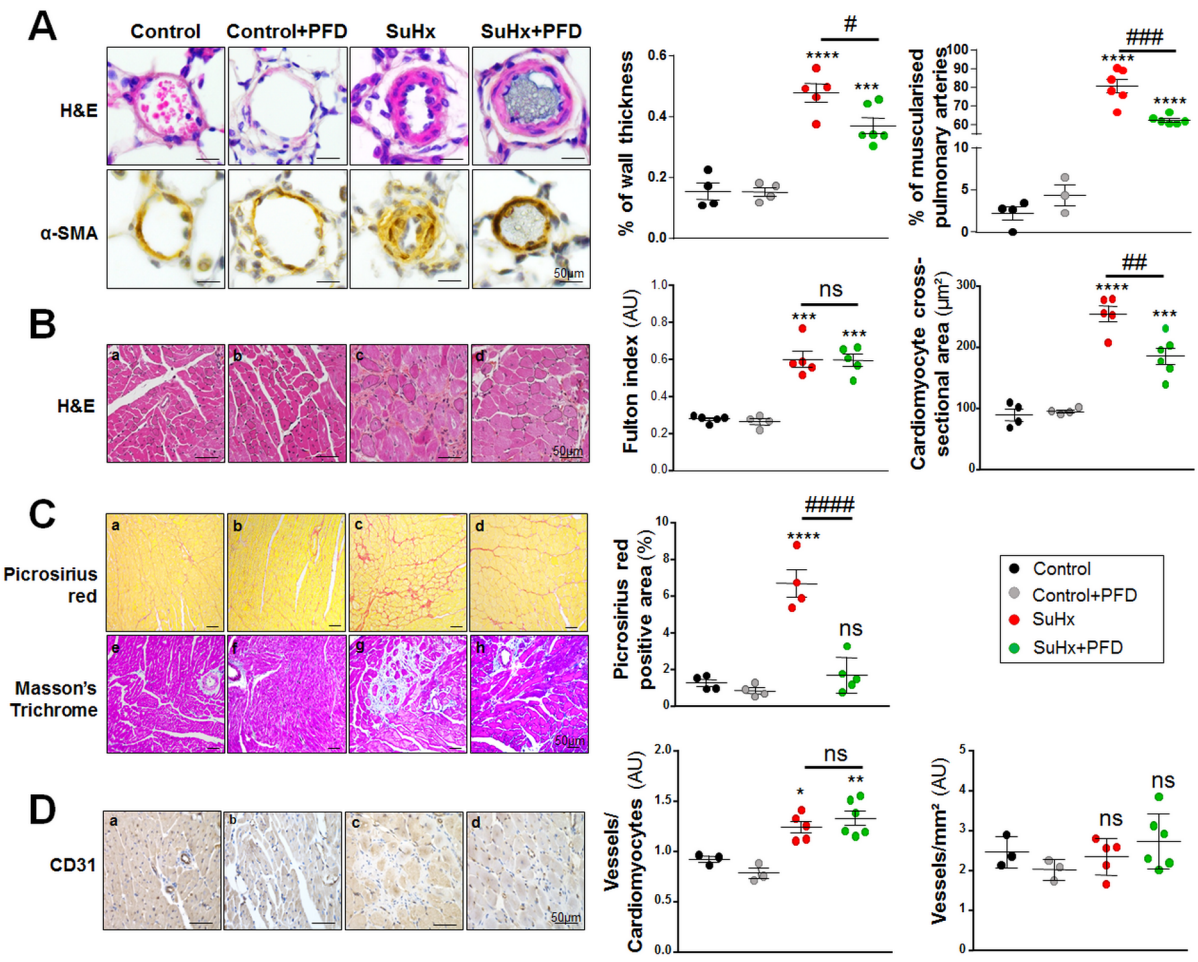
A
Control
Control+PFD
SuHx
SuHx+PFD
H&E
α-SMA
50µm
% of wall thickness
#
% of muscularised pulmonary arteries
###
B
H&E
a
b
c
d
50µm
Fulton index (AU)
ns
Cardiomyocyte cross-sectional area (µm²)
##
C
Picrosirius red
Masson's Trichrome
e
f
g
h
Picrosirius red positive area (%)
####
Control
Control+PFD
SuHx
SuHx+PFD
D
CD31
Vessels/ Cardiomyocytes (AU)
Vessels/mm² (AU)

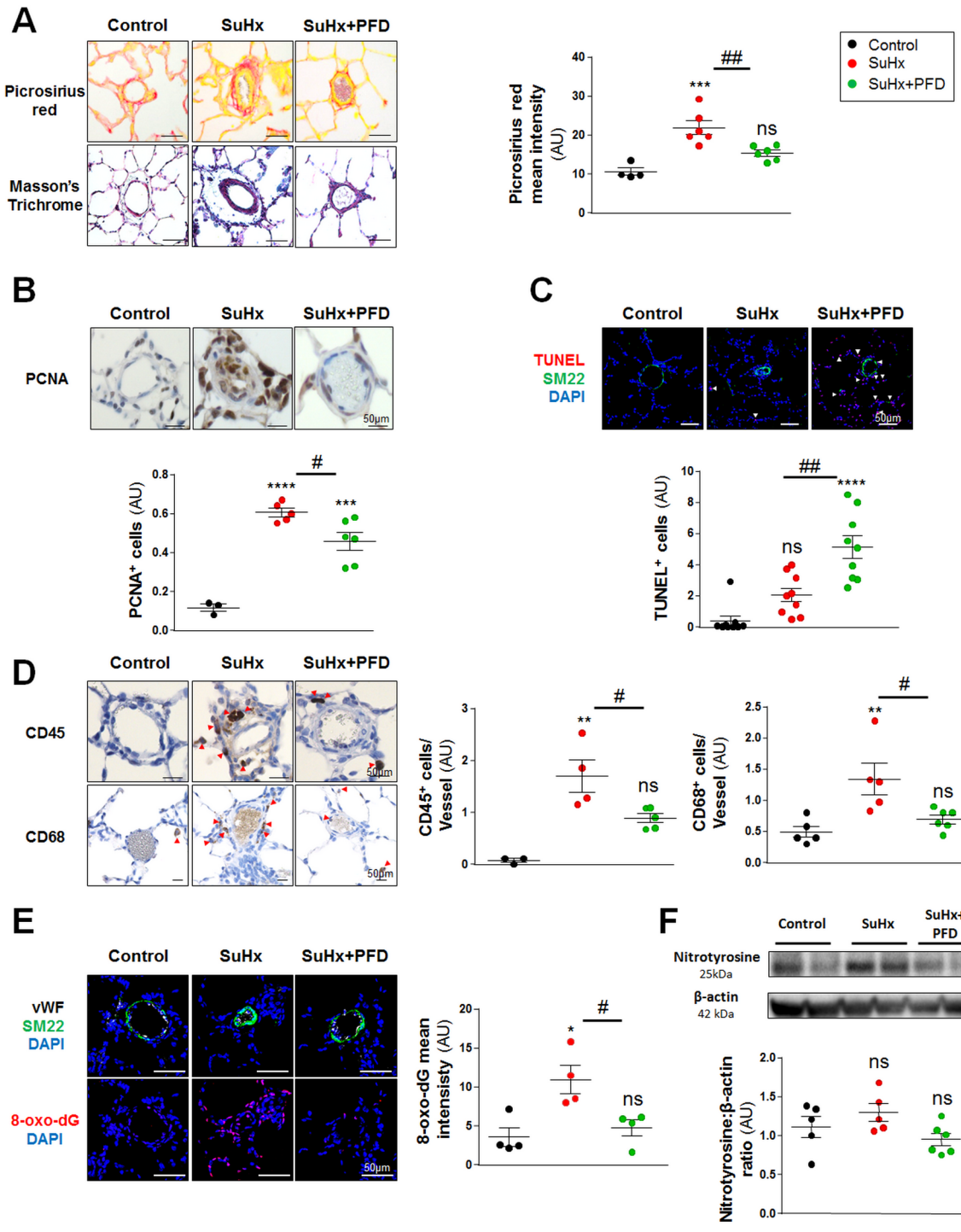
A
Control
SuHx
SuHx+PFD
Picrosirius red
Masson's Trichrome
Picrosirius red mean intensity (AU)
Control
SuHx
SuHx+PFD
B
PCNA
PCNA+ cells (AU)
C
TUNEL
SM22
DAPI
TUNEL+ cells (AU)
D
CD45
CD68
CD45+ cells/ Vessel (AU)
CD68+ cells/ Vessel (AU)
E
vWF
SM22
DAPI
8-oxo-dG
DAPI
8-oxo-dG mean intensisty (AU)
F
Nitrotyrosine
25kDa
β-actin
42 kDa
Nitrotyrosine:β-actin ratio (AU)
50μm
ns

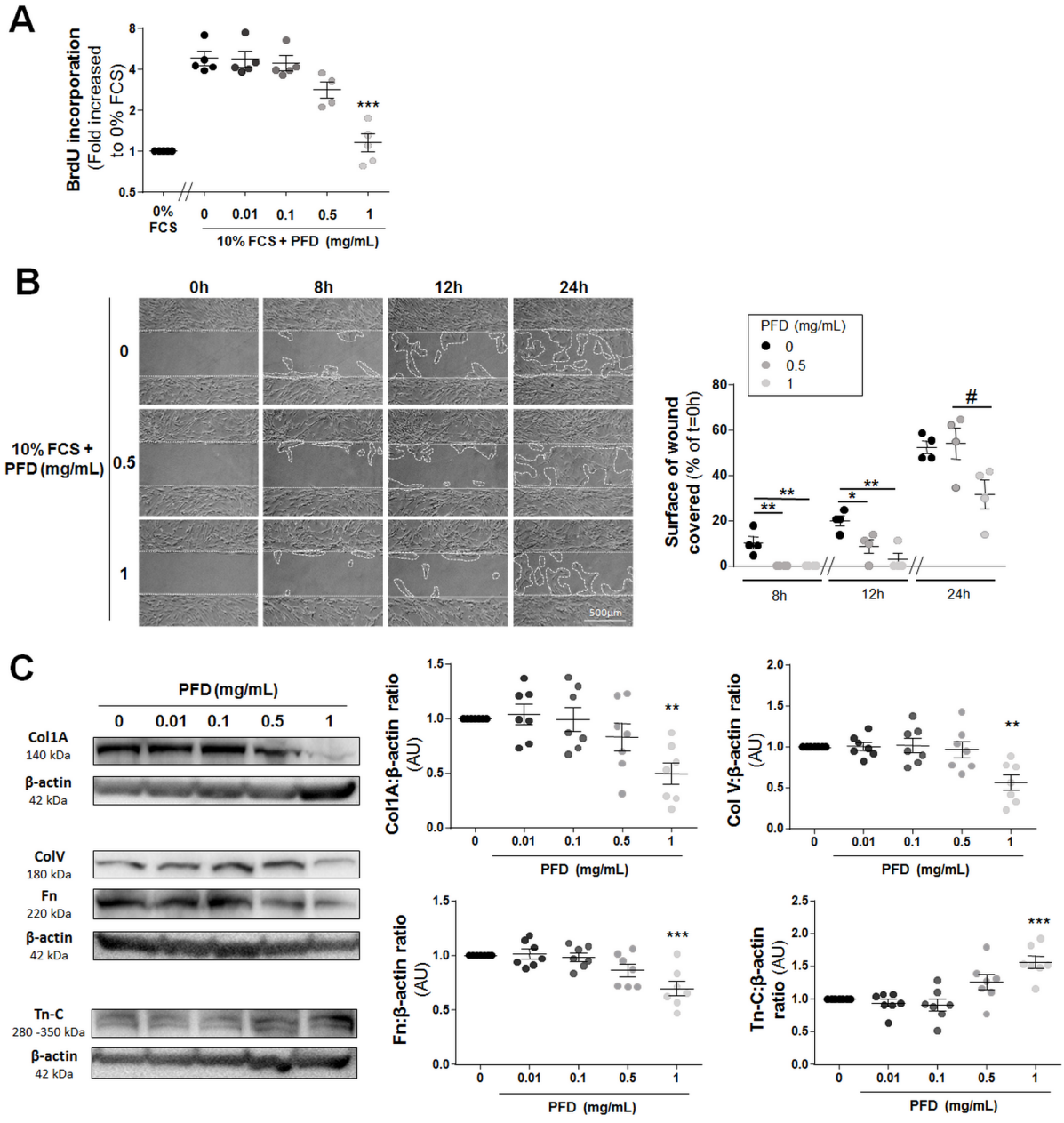
A
BrdU incorporation (Fold increased to 0% FCS)
0% FCS
0
0.01
0.1
0.5
1
10% FCS + PFD (mg/mL)
***
B
0h
8h
12h
24h
10% FCS + PFD (mg/mL)
500µm
PFD (mg/mL)
Surface of wound covered (% of t=0h)
8h
12h
24h
C
PFD (mg/mL)
Col1A
140 kDa
β-actin
42 kDa
ColV
180 kDa
Fn
220 kDa
Tn-C
280 -350 kDa
Col1A:β-actin ratio (AU)
Col V:β-actin ratio (AU)
Fn:β-actin ratio (AU)
Tn-C:β-actin ratio (AU)

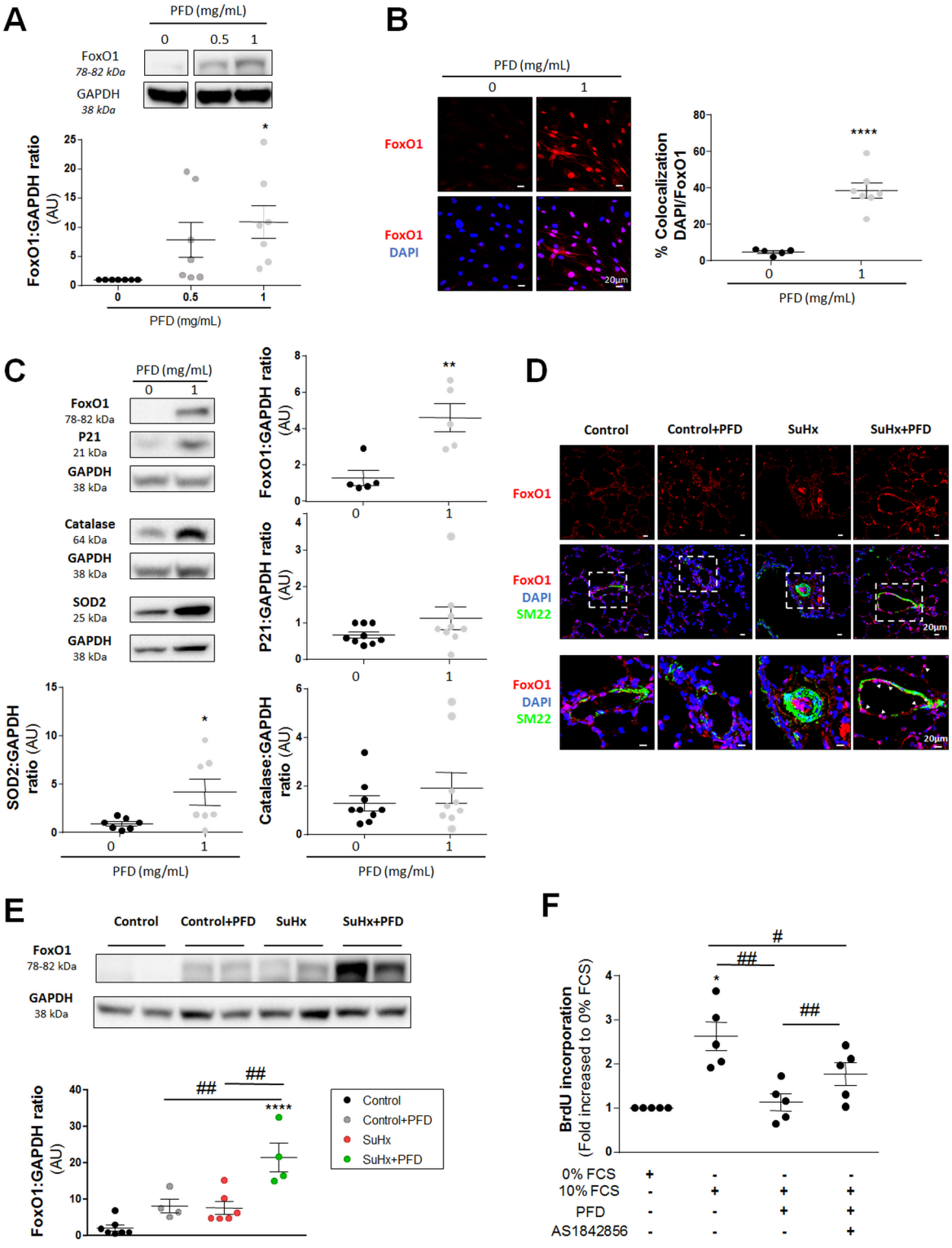
A
PFD (mg/mL)
0
0.5
1
FoxO1
78-82 kDa
GAPDH
38 kDa
FoxO1:GAPDH ratio (AU)
PFD (mg/mL)
B
PFD (mg/mL)
FoxO1
FoxO1
DAPI
20µm
% Colocalization DAPI/FoxO1
PFD (mg/mL)
C
PFD (mg/mL)
FoxO1
78-82 kDa
P21
21 kDa
GAPDH
38 kDa
Catalase
64 kDa
SOD2
25 kDa
FoxO1:GAPDH ratio (AU)
P21:GAPDH ratio (AU)
SOD2:GAPDH ratio (AU)
Catalase:GAPDH ratio (AU)
PFD (mg/mL)
D
Control
Control+PFD
SuHx
SuHx+PFD
FoxO1
DAPI
SM22
20µm
E
Control
Control+PFD
SuHx
SuHx+PFD
FoxO1
78-82 kDa
GAPDH
38 kDa
FoxO1:GAPDH ratio (AU)
Control
Control+PFD
SuHx
SuHx+PFD
F
BrdU incorporation (Fold increased to 0% FCS)
0% FCS
10% FCS
PFD
AS1842856

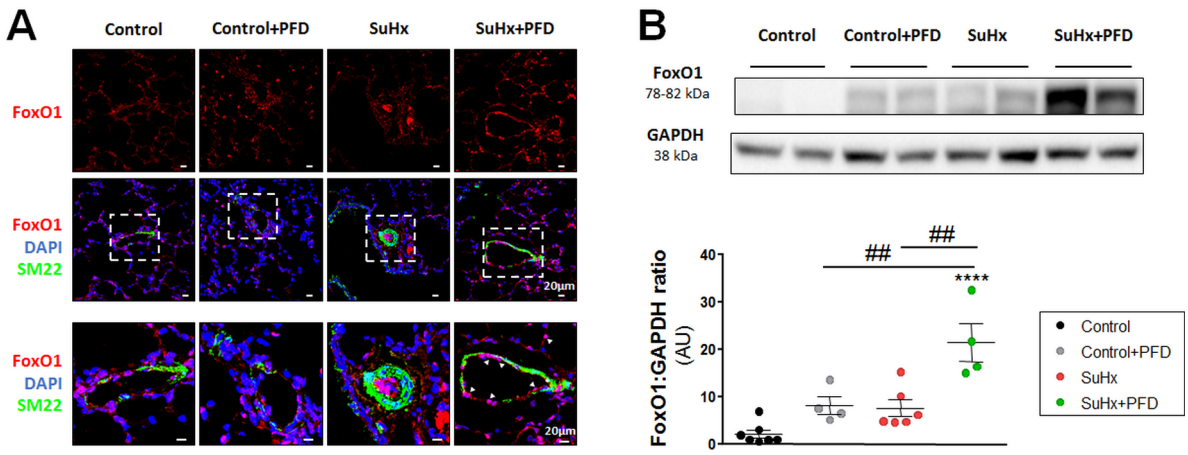
A
Control
Control+PFD
SuHx
SuHx+PFD
FoxO1
FoxO1
DAPI
SM22
20μm
FoxO1
DAPI
SM22
20μm
B
Control
Control+PFD
SuHx
SuHx+PFD
FoxO1
78-82 kDa
GAPDH
38 kDa
FoxO1:GAPDH ratio
(AU)
40
30
20
10
0
##
##
****
Control
Control+PFD
SuHx
SuHx+PFD